

LOCALISATION OF THE MAIN HOM SOURCE IN THE DUSK SIDE OF THE JOVIAN MAGNETOSPHERE

A. Boudouma^{1*} , P. Zarka^{1,2} , F. P. Magalhães¹ , M. S. Marques³ ,
C. K. Louis⁴ , E. Echer⁵ , L. Lamy^{1,6} , and R. Prangé¹ 

*Corresponding author: adam.boudouma@obspm.fr

Citation:

Boudouma et al., 2023, Localisation of the main HOM source in the dusk side of the Jovian magnetosphere, in *Planetary, Solar and Heliospheric Radio Emissions IX*, edited by C. K. Louis, C. M. Jackman, G. Fischer, A. H. Sulaiman, P. Zucca, published by DIAS, TCD, pp. 311–319, doi: 10.25546/103094

Abstract

It was suggested in Zarka et al. (2021) that the most intense Jovian hectometric emissions (HOM) originate from the dusk side of the Jovian magnetosphere. These authors showed that the distribution of the main HOM observed inbound by Cassini-RPWS (i.e. on the dayside of Jupiter) is connected to the “vertex-late” arcs (from the limb rotating away from the observer) of the Jovian left-handed (LH) circularly polarized auroral decametric emissions (DAM). This DAM was identified as “C” emissions from the ground-based observations of the Nançay decameter array (NDA) above 16 MHz. They also suggested, based on the outbound Cassini-RPWS observations alone, that LH HOM observed during the outbound leg of Cassini is connected to the “vertex-early” arcs (from the limb rotating toward the observer) of the LH auroral DAM, called D emissions. We perform here a visual analysis of the vertex-early and vertex-late arcs in the Cassini-RPWS polarized dynamic spectra, for the longitude ranges where the LH HOM is connected to the auroral DAM, to determine the relative proportion of C and D emissions observed when Cassini is inbound and outbound. The results show that at these longitudes, Cassini mainly observes C emissions inbound and D emissions outbound. This confirms that the main HOM is connected to the auroral DAM that originates from the southern dusk hemisphere. A detailed statistical study will follow.

¹ LESIA, Observatoire de Paris, CNRS, PSL, Sorbonne Université, Université de Paris, Meudon, France

² Station de Radioastronomie de Nançay, USN, Observatoire de Paris, CNRS, PSL, Université d’Orléans, Nançay, France

³ Departamento de Geofísica, Universidade Federal do Rio Grande do Norte, Natal, Brazil

⁴ School of Cosmic Physics, DIAS Dunsink Observatory, Dublin Institute for Advanced Studies, Dublin, Ireland

⁵ Instituto Nacional de Pesquisas Espaciais-INPE, São José dos Campos, Brazil

⁶ Aix Marseille Université, CNRS, CNES, LAM, Marseille, France

1 Introduction

The Jovian auroral decametric emissions (DAM) have the shape of arcs in the time-frequency plane and their curvatures can be used to determine whether the source is near the receding (east) or the approaching (west) limb of Jupiter (Hess et al., 2014; Marques et al., 2017): receding limb emissions are called “vertex-late” and approaching limb emissions are “vertex-early”. The right-handed (RH) circularly polarized auroral, vertex-late and -early DAM arcs, respectively called A and B emissions, both originate from the northern hemisphere, whereas their left-handed (LH) circularly polarized equivalents, respectively called C and D emissions, are from the southern hemisphere. They all originate near Jupiter’s limbs because the radio beaming angle is close to 90° (Zarka, 1998): (1) when the observer is near noon in local-time (which is the case for both Cassini’s inbound and ground-based Nançay observations), the vertex-late arcs (A and C) are seen to originate from the dusk sector, whereas the vertex-early arcs (B and D) come from the dawn sector, and (2) when the observer is near midnight in local-time (which is the case for Cassini’s outbound Jupiter observations), the vertex-early arcs (B and D) then originate from the dusk sector, whereas the vertex-late arcs (A and C) come from the dawn sector.

Zarka et al. (2021) showed that the frequency-longitude distribution of the most intense Jovian hectometric emissions (HOM), also called main HOM, observed inbound (i.e. Jupiter’s dayside) by Cassini-RPWS (between ~ 250 - 3000 kHz) is connected to the C emissions (between ~ 3 - 16 MHz), clearly identified as such by the Nançay LH observations (between ~ 16 - 40 MHz). They also suggested based on the outbound (i.e. from Jupiter’s nightside) Cassini-RPWS observations alone (because Nançay can only observe Jupiter’s dayside), that the main LH HOM is connected to the D emissions, but did not prove it. If this is true, it would imply that the most intense HOM mainly originates from the dusk side of the Jovian magnetosphere. More specifically, they compared the stacked longitude-frequency distributions of LH auroral emissions observed by Cassini-RPWS along the inbound leg of Jupiter’s flyby (day-of-year 2000-275 to 2000-345) below 16 MHz with the DAM occurrence probability in the 29-year Nançay data base (Marques et al., 2017) above 16 MHz. They showed that the Cassini inbound LH HOM is the low-frequency extent of the C emissions, whereas the Cassini outbound LH HOM is the low-frequency extent of LH auroral DAM that remains to be identified, but that they suggested to be D emission.

In order to test Zarka et al. (2021) suggestions, here we performed a visual analysis of the auroral DAM arcs curvatures in the Cassini-RPWS inbound and outbound dynamic spectra. The aim is to quantify, for the longitudes where the main HOM is connected to the LH auroral DAM, the relative proportion of C and D emissions on the dayside and the nightside. The A and B emissions are not studied here as the HOM auroral DAM connections are much clearer in LH and also because their arcs curvatures are not clearly visible on the Cassini-RPWS dynamic spectra below 16 MHz. Section 2 presents the distributions of LH radio flux density as a function of observer’s longitude and frequency, adapted from Zarka et al. (2021), the longitude ranges within which we examine RPWS dynamic spectra and the criteria used to label the arcs depending on their vertex. Section 3 displays the Cassini’s inbound and outbound vertex-late/-early

arc occurrences and Section 4 summarizes and discusses the results.

2 Cassini-RPWS LH auroral DAM analysis

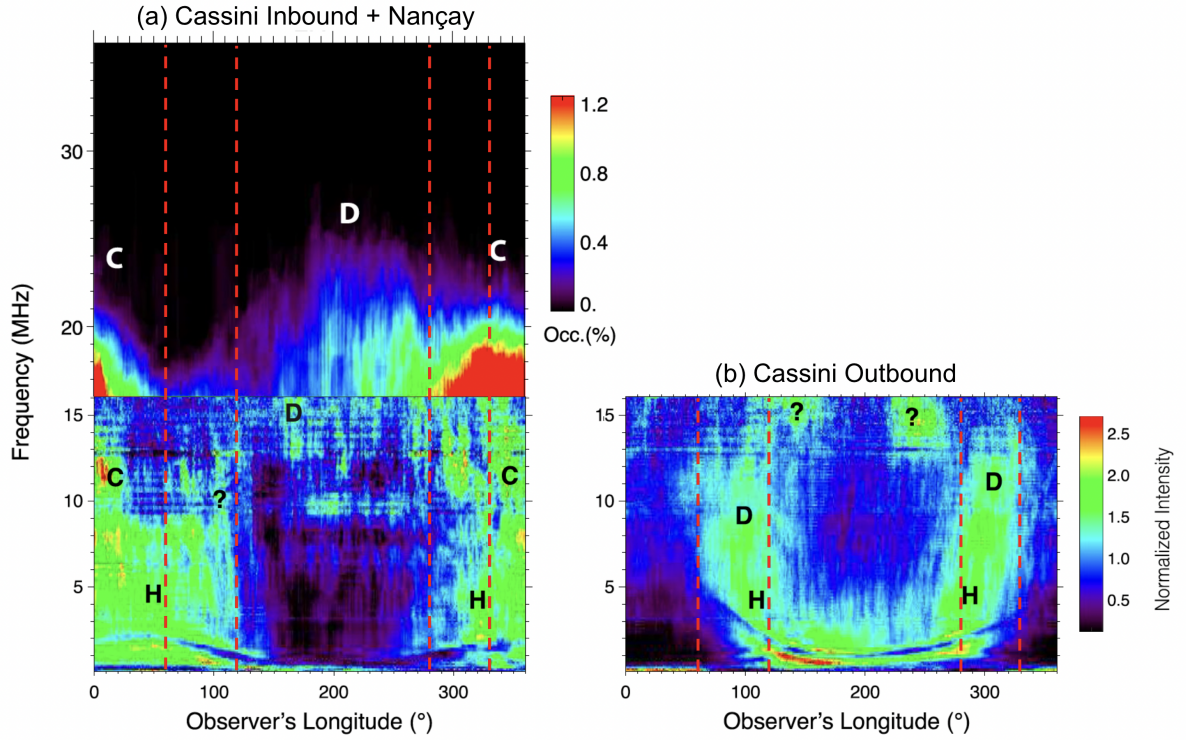


Figure 1: Frequency-longitude distributions of the Jovian LH auroral components, from (a) merged inbound Cassini data below 16 MHz and Nançay data above 16 MHz (Marques et al., 2017) and (b) outbound Cassini data below 16 MHz, both with a linear frequency scale adapted from (Zarka et al., 2021). Longitude bins are 1° wide. The intensity scale is in relative units of average flux density at each frequency for Cassini and occurrence probability for Nançay data. Question marks “?” correspond to DAM components not unambiguously identified.

Figure 1, adapted from Zarka et al. (2021) (Figure 3d and 9a), displays (a) a composite frequency versus observer’s longitude (CML) distribution of the LH Jovian auroral components from Jupiter’s dayside built from Cassini’s inbound observations that cover the 5 kHz - 16,125 kHz frequency range and Nançay data were recorded above 15 MHz; (b) frequency-longitude distributions of the Jovian auroral components from Jupiter’s night-side in the Cassini’s outbound observations alone. The frequency scales are linear. The color scales are different for Nançay (occurrence probabilities) and Cassini (normalized intensities). As noted in Zarka et al. (2021) :

- Inbound, C and D components are clearly identified on the LH polarized Cassini and Nançay observations panel 1a. The C emissions (annotated C) are continuously connected to the HOM emissions (annotated H) for longitudes in ranges $0-120^\circ$ and $280-360^\circ$ while D emissions (annotated D) are detached from the HOM.

- Outbound, HOM emissions are continuously connected with an unidentified auroral DAM emission on the LH polarized Cassini's outbound observation panel 1b, that was suggested to be D emission (annotated D) for longitudes in the ranges $\sim 60^\circ$ - 150° and ~ 250 - 330° .

We focus on Cassini's near noon (local time between $\sim 10\text{h}45$ and $15\text{h}00$) inbound observations (day-of-year 2000-275 to 2000-360) and near midnight (local time between $\sim 20\text{h}30$ and $21\text{h}00$) outbound observations (day-of-year 2000-390 to 2000-475) as they correspond to time ranges when the observing geometry restricted the RPWS's visibility to dawn-dusk auroral DAM (cf. Figure 1 of Zarka et al. (2021)).

We examine the Cassini-RPWS dynamic spectra and identify the LH auroral DAM arc curvatures for longitudes that cover both identified HOM-C inbound and suggested HOM-D outbound, between longitudes of 60° - 120° and (2) 280° - 330° , bounded by red dashed lines on Figure 1.

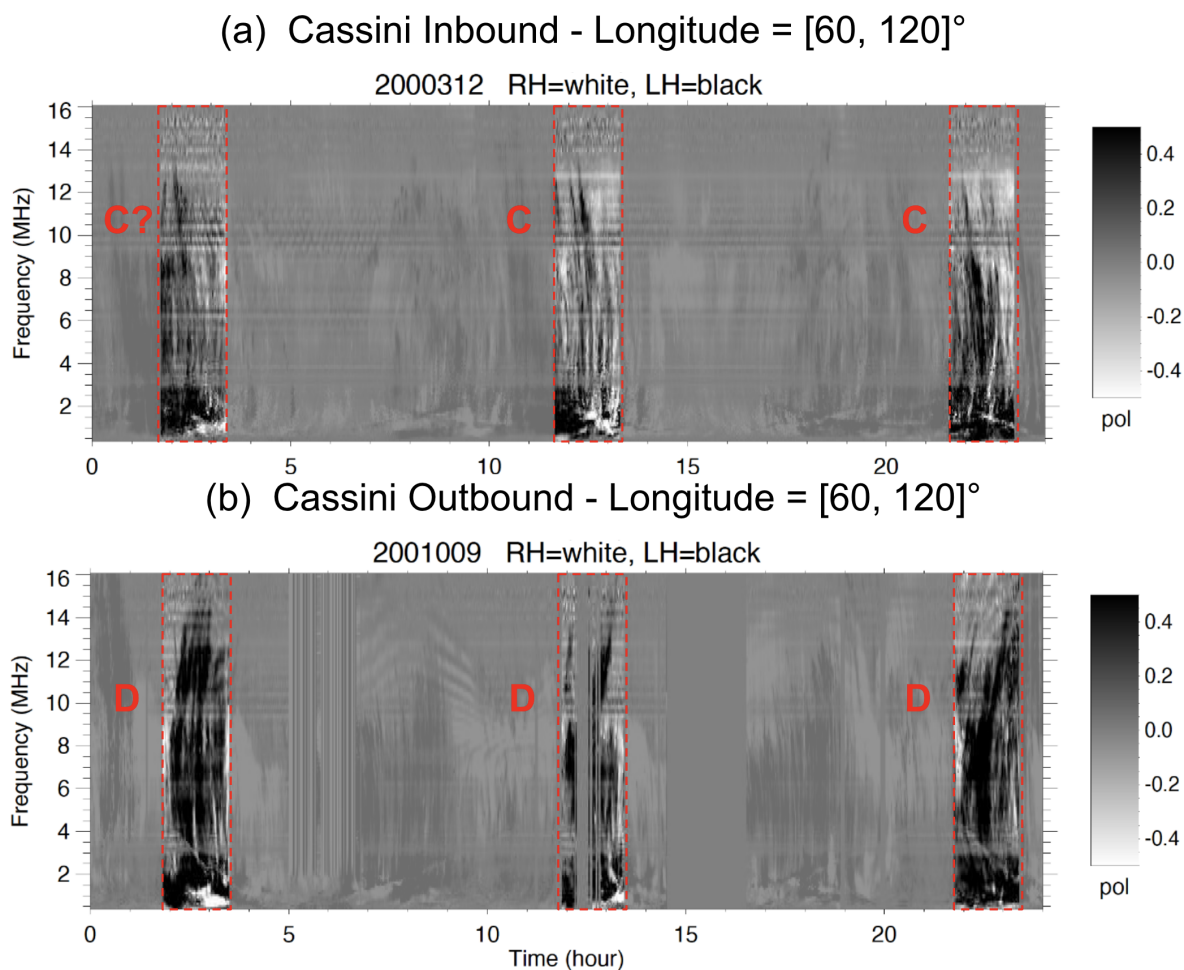


Figure 2: Example of two 24-hour Cassini-RPWS dynamic spectra from (a) the inbound day-of-year 2000-312 (i.e. 07/11/2000) and (b) outbound day-of-year 2001-009 (i.e. 09/01/2001), respectively displaying vertex-late and vertex early DAM arcs. The grey scale labeled “pol” represents the circular polarization V (saturated at ± 0.5). The red boxes are the selections corresponding to the longitude range 60° - 120° selections in longitudes. For clarity, the parts outside the red boxes have a reduced contrast.

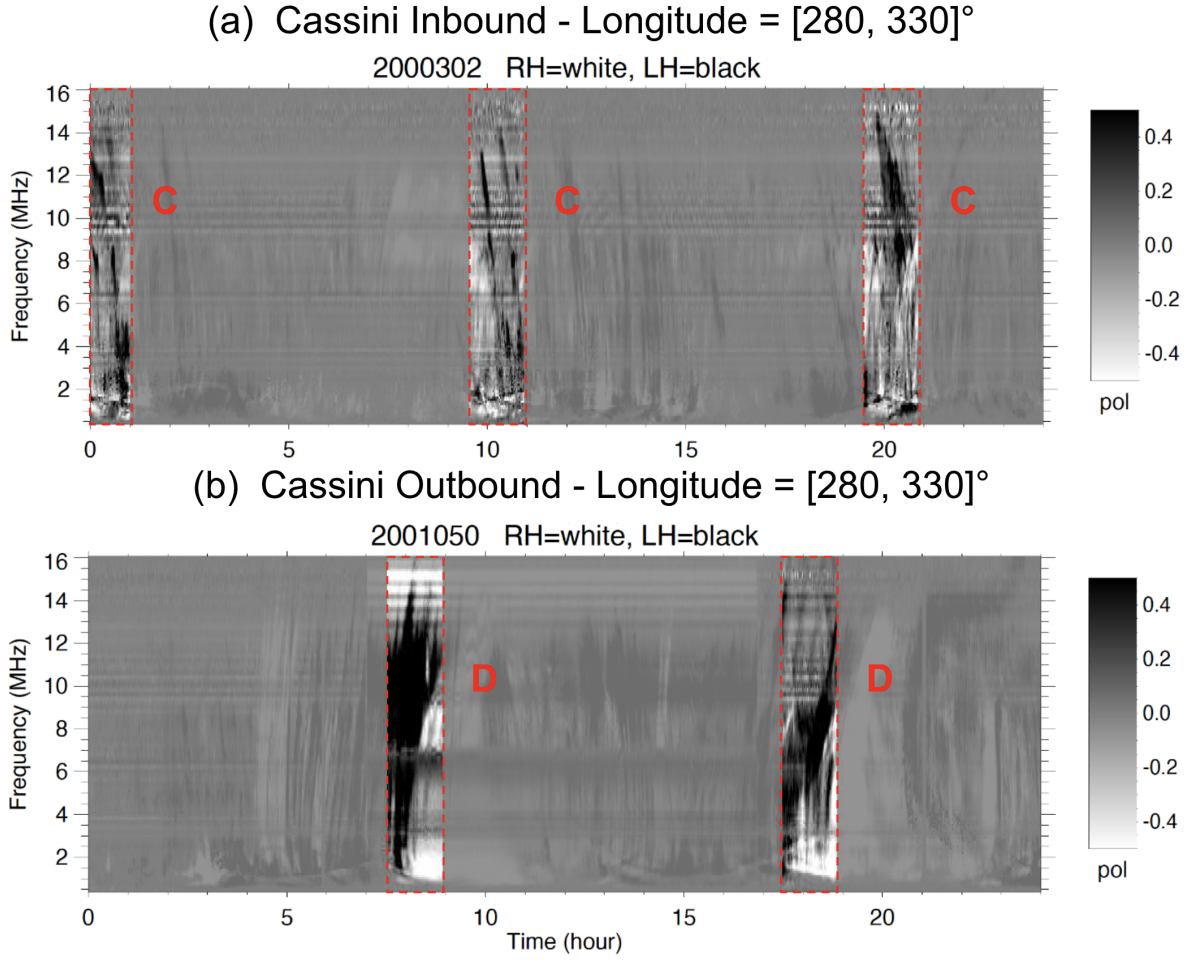


Figure 3: Same as Figure 2 for (a) inbound day-of-year 2000-302 (i.e. 28/10/2000) and (b) outbound day-of-year 2001-050 (i.e. 19/02/2001) for the longitudes 280° - 330° .

We performed a visual analysis of the Cassini-RPWS inbound and outbound dynamic spectra by identifying the predominant curvature of the LH auroral DAM in each selected interval (either 60° - 120° or 280° - 330°). We label each selected interval as described on Table 1.

Table 1: Arcs labeling rule.

Label	Description
C	Clear vertex-late arcs predominance over the vertex-early arcs
C?	Uncertain vertex-late arcs predominance over the vertex-early arcs
D	Clear vertex-early arcs predominance over the vertex-late arcs
D?	Uncertain vertex-early arcs predominance over the vertex-late arcs
X	Not possible to distinguish arc curvature or predominance

Figures 2 and 3 display representative examples of the analyzed 24-hour Cassini-RPWS dynamic spectra, for inbound and outbound periods respectively, selected for the longitudes 60° - 120° and 280° - 330° . The frequency range covers 5 kHz - 16,125 kHz in linear

scale. The intensity values correspond to the saturated circular polarization fraction V ($-0.5 \leq V \leq 0.5$) with $V = 0.5$ (black color) corresponding to LH polarization and $V = -0.5$ (white color) to RH polarization. As this study focuses on the LH polarized emissions, we will look exclusively at the emissions colored in black. Each longitude selection corresponds to a time selection on the dynamic spectra. These regions are highlighted by the dashed red boxes. We purposely attenuated the contrast of the dynamic spectra outside the selected data intervals, for clarity. Figures 2 and 3 both clearly reveal (a) predominant vertex-late arcs (labelled “C”) for the inbound selections and (b) predominant vertex-early arcs (labelled “D”) for the outbound selections. Only the first box in panel (a) of Figure 2 between 1h40 and 3h20 is labelled “C?”, because the main vertex-late arc is preceded by vertical or slightly vertex-early emissions between 1h40 and 2h10. The situation depicted in Figures 2 and 3, where we have vertex-late arcs predominance inbound and vertex-early arcs predominance outbound, for both longitude selections, is typical of the whole dataset. Occurrences are quantitatively investigated in the following section.

3 Inbound and outbound occurrences of C and D auroral DAM

In this section we compare the occurrence of vertex-early and vertex-late arc events identified using the method described in Section 2. This will tell us which type of arc is statistically prevalent inbound and outbound for the longitude ranges 60° - 120° and 280° - 330° .

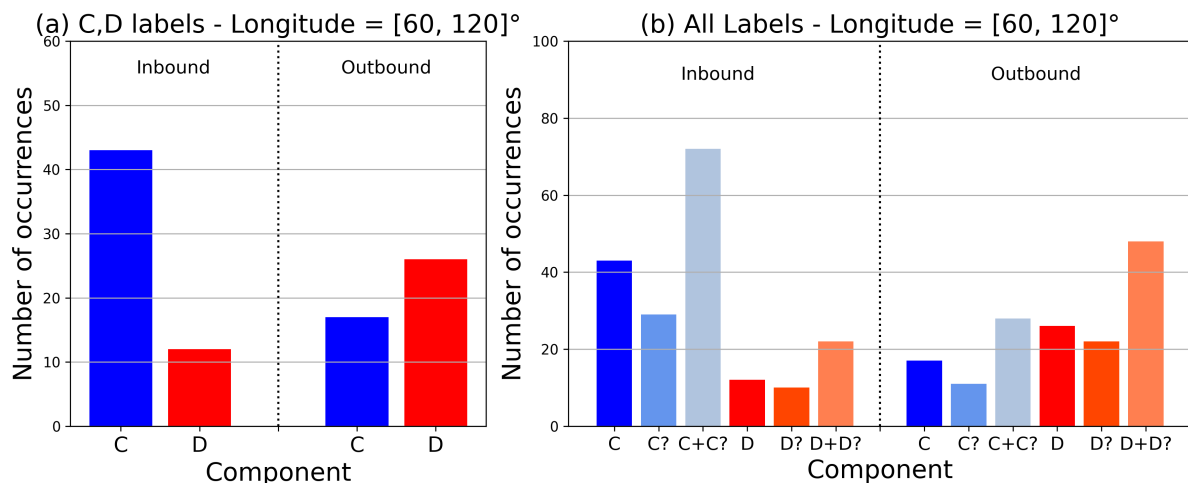


Figure 4: Histograms of the predominant LH auroral DAM arcs curvature observed on the Cassini-RPWS circular polarization dynamic spectra in the longitude range 60° - 120° . Panel (a) displays the number of occurrences only for the selections labelled as clear vertex-late “C” or vertex-early “D” predominance. Panel (b) displays the number of occurrences of clear vertex-late “C” or vertex-early “D” arc predominance, “uncertain” vertex-late “C?” or vertex-early “D?” identifications, and the sums of occurrences “C+C?” and “D+D?”.

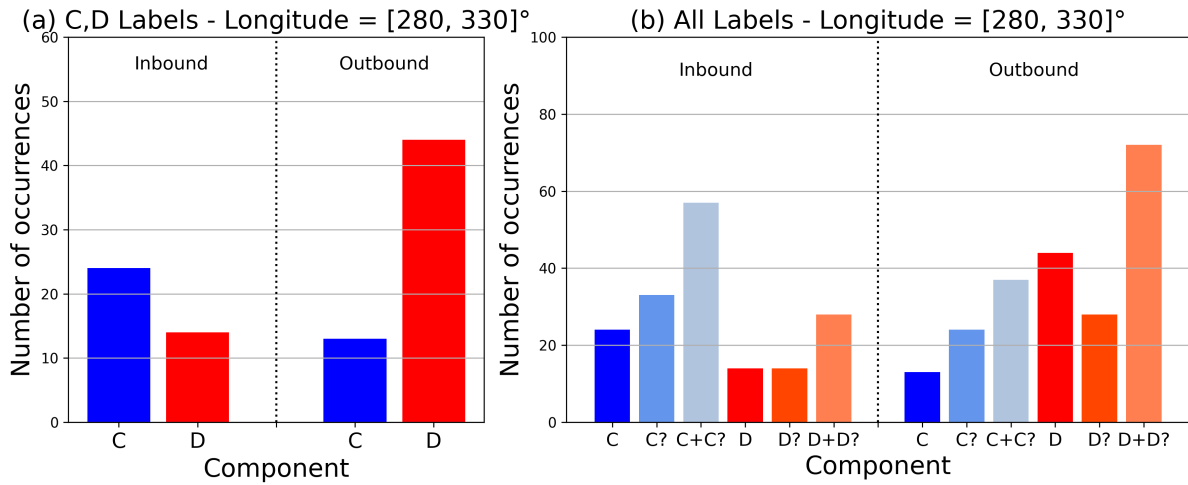


Figure 5: Same as Figure 1 for the longitude range 280° - 330° .

Figure 4 displays occurrence histograms for the longitude range 60° - 120° . The vertex-late arcs are clearly prevalent inbound with 43 “C” versus 10 “D” occurrences, whereas the vertex-early arcs are prevalent outbound with 18 “C” versus 26 “D” occurrences. The behavior is similar if we take into account the selections with an uncertain predominance with 71 “C+C?” occurrences versus 22 “D+D?” occurrences inbound and 33 “C+C?” occurrences versus 50 “D+D?” occurrences outbound. We note that the number of “D” occurrences inbound is close to the number of “C” occurrences outbound, but the number of “D” occurrences outbound is almost two times lower than the number of “C” occurrences inbound.

Figure 5 displays similar histograms for the longitude range 280° - 330° . The vertex-late arcs are clearly prevalent inbound with 24 “C” versus 14 “D” occurrences, whereas the vertex-early arcs are prevalent outbound with 14 “C” versus 49 “D” occurrences. The behavior is similar if we take into account the selections with an uncertain predominance with 57 “C+C?” occurrences versus 28 “D+D?” occurrences inbound and 39 “C+C?” occurrences versus 84 “D+D?” occurrences outbound. Inversely to Figure 4, the number of “D” occurrences inbound is close to the number of “C” occurrences outbound, but the number of “C” occurrences inbound is almost two times lower than the number of “D” occurrences outbound.

For both longitude regions, the vertex-late arcs are prevalent inbound, whereas the vertex-early arcs are prevalent outbound. It confirms that the LH HOM emissions are mainly connected to the C emissions inbound and D emissions outbound. We also observe an inbound and outbound occurrence asymmetry between the prevalent arcs, inverted between the longitude selections 60° - 120° (almost twice fewer occurrences for the outbound prevalent component) and 280° - 330° (almost twice fewer occurrences for the inbound prevalent component).

4 Discussion and perspectives

We have identified two longitude regions of interest from the frequency-longitude distributions of the Cassini-RPWS Jupiter's flyby and Nançay database, 60° - 120° and 280° - 330° , where the main HOM is connected to the C emission inbound and unidentified LH polarized auroral DAM outbound.

We have analyzed Cassini-RPWS polarization dynamic spectra for these two longitude ranges, identifying the prevalent LH arc curvatures inbound and outbound. We have shown for both longitude ranges 60° - 120° and 280° - 330° that the vertex-late arcs are mainly prevalent inbound, whereas the vertex-early arcs are prevalent outbound. This means that, the prevalent component originates from the receding limb when seen from the day-side, and from the approaching limb on the nightside. This interpretation agrees with the suggestion by Zarka et al. (2021) that the unidentified auroral DAM in Cassini's outbound observations is D emission. We also confirm that the most intense HOM observed in LH polarization is connected to auroral DAM that originate from the southern dusk hemisphere. This result is consistent with observations from Bonfond et al. (2015) which have indicated that the FUV Jovian aurorae are 3.3 times brighter on the dusk sector than on the dawn sector. This can also be related to the structure of the dusk side magnetosphere where the plasma disc is thicker and more active (Kivelson & Southwood, 2005). Finally the prevalence of the dusk emissions is consistent with Hess et al. (2014), who noted that they are triggered by both fast-forward and fast-reverse shocks of the solar wind, whereas dawn emissions are only triggered by fast-reverse shocks. However, the inbound and outbound occurrence asymmetry of the prevalent component and their inversion between the longitudes 60° - 120° and 280° - 330° , remains to be understood.

We have limited this study to the analysis of the prevalent LH auroral DAM component for two longitude regions from the frequency-longitude distributions. However, Cassini-RPWS observations (e.g. Figures 3 & 9 from Zarka et al. (2021)) clearly show that HOM is both connected and distinct from auroral DAM. For southern emission (C and D), HOM seems more merged with DAM than for northern emission (A and B). We think that the partly distinct character of HOM relative to DAM may come from:

1. Its beaming: DAM is emitted within the first $\sim 0.5 R_j$ above the surface of Jupiter, while HOM (e.g. in the range 0.3-7 MHz) is emitted at 1.5-4.5 R_j jovicentric distance; this geometrically enables larger beaming variation effects.
2. The cyclotron-maser instability energy source: the loss-cone in the upgoing electron distribution that drives cyclotron-maser to produce DAM might be exhausted in some cases at the altitude of HOM.

Extensive studies on the subject are needed to examine in-depth the implication of these two effects. A future detailed statistical study in longitude will be realized by labeling each auroral DAM arc A, B, C and D, observed by Cassini-RPWS over the entire Jupiter flyby with help of the SPACE labeling tool (Louis et al., 2022).

Acknowledgments

C. K. Louis' work at the Dublin Institute for Advanced Studies was funded by the Science Foundation Ireland Grant 18/FRL/6199.

References

- Bonfond B., et al., 2015, The far-ultraviolet main auroral emission at Jupiter - Part 1: Dawn-dusk brightness asymmetries, *Annales Geophysicae*, 33, 1203
- Hess S., Echer E., Zarka P., Lamy L., Delamere P., 2014, Multi-instrument study of the jovian radio emissions triggered by solar wind shocks and inferred magnetospheric subcorotation rates, *Planetary and Space Science*, 99, 136
- Kivelson M. G., Southwood D. J., 2005, Dynamical consequences of two modes of centrifugal instability in Jupiter's outer magnetosphere, *Journal of Geophysical Research: Space Physics*, 110, A12209
- Louis C., et al., 2022, The "SPectrogram Analysis and Cataloguing Environment" (SPACE) labelling tool, *Frontiers in Astronomy and Space Sciences*, 9, 1001166
- Marques M. S., Zarka P., Echer E., Ryabov V. B., Alves M. V., Denis L., Coffre A., 2017, Statistical analysis of 26 yr of observations of decametric radio emissions from Jupiter, *Astronomy & Astrophysics*, 604, A17
- Zarka P., 1998, Auroral radio emissions at the outer planets: Observations and theories, *Journal of Geophysical Research*, 103, 20159
- Zarka P., Magalhães F. P., Marques M. S., Louis C. K., Echer E., Lamy L., Cecconi B., Prangé R., 2021, Jupiter's auroral radio emissions observed by cassini: Rotational versus solar wind control, and components identification, *Journal of Geophysical Research: Space Physics*, 126, e2021JA029780